

Learning Spectral-Decomposed Tokens for Domain Generalized Semantic Segmentation

Jingjun Yi
rsjingjuny@whu.edu.cn
Wuhan University
Wuhan, China

Qi Bi
q_bi@whu.edu.cn
Wuhan University
Wuhan, China

Hao Zheng*
howzheng@tencent.com
Tencent Youtu Lab
Shenzhen, China

Haolan Zhan
haolan.zhan@monash.edu
Monash University
Clayton, Australia

Wei Ji
wei.ji@yale.edu
Yale University
New Haven, United States

Yawen Huang
yawenhuang@tencent.com
Tencent Youtu Lab
Shenzhen, China

Yuxiang Li*
yuxiang.li@sr.gxmu.edu.cn
Guangxi Medical University
Nanning, China

Yefeng Zheng
yefengzheng@tencent.com
Westlake University
Hangzhou, China
Tencent Youtu Lab
Shenzhen, China

Abstract

The rapid development of Vision Foundation Model (VFM) brings inherent out-domain generalization for a variety of down-stream tasks. Among them, domain generalized semantic segmentation (DGSS) holds unique challenges as the cross-domain images share common pixel-wise content information but vary greatly in terms of the style. In this paper, we present a novel Spectral-decomposed Token (SET) learning framework to advance the frontier. Delving into further than existing *fine-tuning token & frozen backbone* paradigm, the proposed SET especially focuses on the way learning style-invariant features from these learnable tokens. Particularly, the frozen VFM features are first decomposed into the phase and amplitude components in the frequency space, which mainly contain the information of content and style, respectively, and then separately processed by learnable tokens for task-specific information extraction. After the decomposition, style variation primarily impacts the token-based feature enhancement within the amplitude branch. To address this issue, we further develop an attention optimization method to bridge the gap between style-affected representation and static tokens during inference. Extensive cross-domain experiments show its state-of-the-art performance.

CCS Concepts

• Computer Vision; • Representation Learning;

*Hao Zheng and Yuxiang Li are the corresponding authors.

Permission to make digital or hard copies of all or part of this work for personal or classroom use is granted without fee provided that copies are not made or distributed for profit or commercial advantage and that copies bear this notice and the full citation on the first page. Copyrights for components of this work owned by others than the author(s) must be honored. Abstracting with credit is permitted. To copy otherwise, or republish, to post on servers or to redistribute to lists, requires prior specific permission and/or a fee. Request permissions from permissions@acm.org.

MM '24, October 28-November 1, 2024, Melbourne, VIC, Australia

© 2024 Copyright held by the owner/author(s). Publication rights licensed to ACM.

ACM ISBN 979-8-4007-0686-8/24/10

<https://doi.org/10.1145/3664647.3680906>

Keywords

Domain Generalized Semantic Segmentation, Frequency Decoupling, Token Tuning, Vision Foundation Model

ACM Reference Format:

Jingjun Yi, Qi Bi, Hao Zheng, Haolan Zhan, Wei Ji, Yawen Huang, Yuxiang Li, and Yefeng Zheng. 2024. Learning Spectral-Decomposed Tokens for Domain Generalized Semantic Segmentation. In *Proceedings of the 32nd ACM International Conference on Multimedia (MM '24)*, October 28-November 1, 2024, Melbourne, VIC, Australia. ACM, New York, NY, USA, 10 pages. <https://doi.org/10.1145/3664647.3680906>

1 Introduction

Semantic segmentation is a fundamental task in computer vision [25, 28, 41]. Most of these methods assume that the unseen target domains in the inference stage share the independent and identical distribution (i.i.d.) with the accessed source domain in the training stage. In the real-world applications like autonomous driving, this assumption usually does not necessarily hold. As a matter of fact, large style variations between the source and unseen target domains can be witnessed due to many shifting factors such as urban landscape, weather, and lighting conditions [12, 36, 54].

Domain generalized semantic segmentation (DGSS) is the task to address this challenge, in which the segmentation models are trained only on the source domain but inferred on arbitrary unseen target domains [3, 4, 18]. Before the Vision Foundational Model (VFM) era, extensive efforts have been made on DGSS, which focus on either style decoupling [3, 4, 14, 18, 45, 46] or style augmentation [24, 33, 70, 72]. However, the representation ability of the scene content (e.g., semantics) itself, which is relatively stable between different domains, remains less explored. In recent years, VFMs (e.g., CLIP [50], DALL-E [51], DINOv2 [40], and SAM [31]) have significantly advanced a variety of vision tasks. The inherited generalization ability of VFM from large-scale image pre-training [32] has great potential to be harnessed for DGSS.

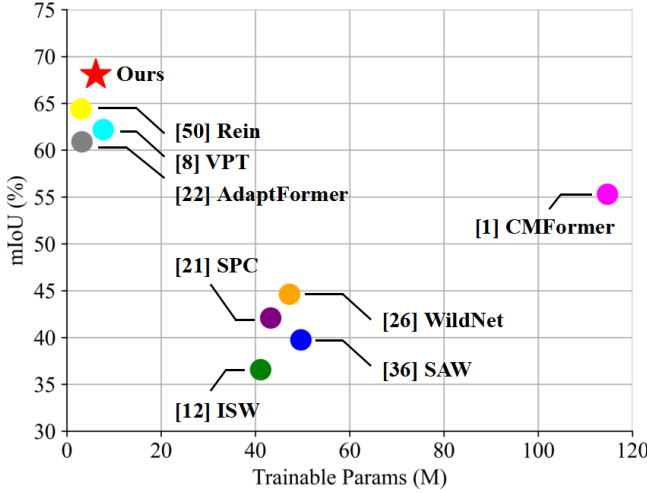


Figure 1: Segmentation performance on unseen target domain (in mIoU, %) v.s. trainable parameter number (in million, M). GTAV [52] is used as the source domain and CityScapes [16] is used as unseen target domain. The proposed SET shows state-of-the-art performance with little trainable parameters.

Recent works show that, in the context of DGSS (Fig. 1), fine-tuning VFM with learnable tokens yields better generalization than the one with full parameter tuning [60]. However, the key challenge of DGSS, i.e., the domain gap caused by the style variation, remains unaddressed. Hence, we naturally raise an open research question: *how to learn style-invariant representation by fine-tuning VFMs?* Spectral decomposition has been long acknowledged effective to handle the style and content information separately in the context of domain generalization [22, 35, 62, 64, 68], where the style/content information highly rests in the high-/low- frequency component [58]. This further leads to our second research question: *how to design a frequency-space-based method to effectively composite the style and content information from the VFM features?*

In this paper, we propose a novel Spectral-decomposed Token (SET) learning scheme to address this challenge. Fast fourier transform (FFT) [5] is implemented to decompose the image feature from the previous frozen VFM layer to the amplitude and phase components. As shown in Fig. 2, the phase component, which contains more low-frequency component on the scene content, is relatively stable despite the cross-style variation [47, 63]. In contrast, the amplitude component, which has more high-frequency component on the styles [8, 64], can be rather unstable when handling images from different domains. Therefore, the token features on the amplitude component deserves more attentions in domain generalization.

To this end, we design a token-based feature enhancement pipeline which extracts task-specific information and adjusts the spectral-decomposed features in amplitude and phase branches separately. Learnable tokens capture task-relevant features within each branch, and enhance the original feature representations based on their similarities. During inference, these tokens are fixed. However, since the amplitude component is susceptible to style variation, the enhancement process in the amplitude branch can become unstable

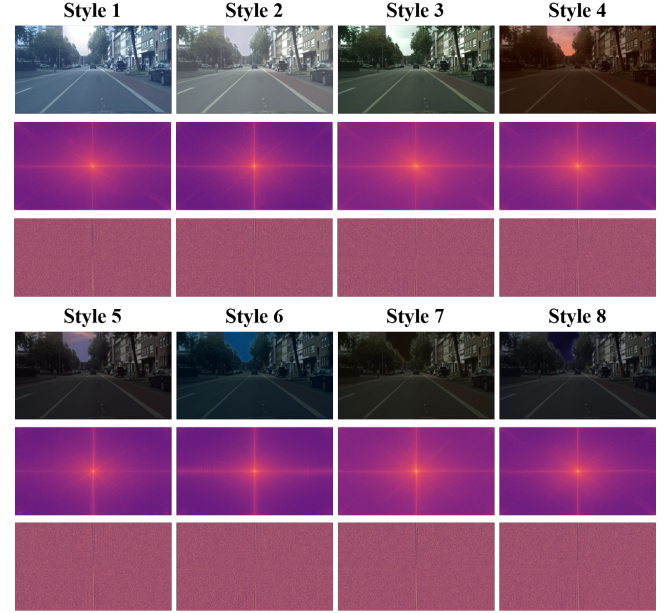


Figure 2: A toy example on how different styles of a driving scene (left row) impact the amplitude (second row) and the phase component (third row). As the styles change, the phase component remains stable, while the amplitude adjusts correspondingly. Thus, the amplitude component provides a feasible path to inspect the cross-domain style variation.

due to the fluctuating representation and static tokens. Therefore, we further propose an attention optimization method to make the token-based enhancement more robust to style changes. Finally, the enhanced amplitude and phase components are projected back to the spatial space and input to the subsequent layer.

Our contributions are summarized as follows:

- We propose a novel spectral-decomposed token learning (SET) scheme for DGSS. It harnesses the style-invariant properties for VFM.
- The proposed SET, consisting of three key steps, namely, spectral decomposition, learning spectral tokens, and attention optimization in the amplitude branch, can be seamlessly integrated into existing VFMs in a trainable manner.
- Extensive experiments show the proposed SET outperforms the VFM based state-of-the-art by up to 1.66% and 3.12% mIoU on unseen CityScapes and ACDC-snow domains.

2 Related Work

2.1 Domain Generalization

Domain generalization focused on the scenarios where the target domain is unavailable during training. Various approaches have been proposed in the past decade. A straight-forward research line is to design variations of the normalization techniques [15, 37, 55], which are simple and effective to enhance the representation robustness to style robustness. Additionally, extensive advanced techniques, to name a few, adversarial training [17], domain alignment

[11, 56], meta-learning [9, 49], data augmentation [57, 67, 71], self-supervised learning [6], and regularization techniques [1, 30, 59], have been adapted to learn the domain-invariant representation.

However, the above works usually focus on the non task-specific settings, not especially devised for DGSS. In DGSS, the key challenge lies in that the cross-domain images share common content information (i.e., semantics) but vary greatly in terms of the style variation (e.g., urban landscape, environment dependencies).

2.2 Vision Foundation Models

Foundation model is a new paradigm for deep learning. Its key idea is to pre-train a deep network on a board set of unlabeled images, which has a strong representation ability to be fine-tuned on a variety of down-stream tasks. This paradigm firstly emerges in the field of Natural Language Processing (NLP), and later also draws increasingly attention in the community of computer vision. For simplicity, in the following text, the foundation models in the computer vision field is termed as Vision Foundation Model (VFM).

Here, we review several typical VFMs in the past few years: Contrastive Language-Image Pre-Training (CLIP) [50] acquires high-fidelity visual representations via contrastive learning with large-scale image-text pairs. Masked Auto-encoder (MAE) [20] employs a masked image modeling framework to derive latent image representations. Segment Anything Model (SAM) [31] pioneers a promptable model pre-trained on a diverse dataset for segmentation tasks. Explore the limits of Visual representation at sAlE (EVA) [19] merges Masked Image Modeling pre-training with CLIP’s vision features as the target of pretext tasks. Self-Distillation with NO labels (DINO) [40] pre-trains the deep model on extensive, meticulously curated datasets without explicit supervision.

To summarize, these VFMs have shown great successes on improving a variety of downstream tasks, underscoring their remarkable generalization capabilities. Nevertheless, an in-depth exploration of their effectiveness in the specialized realm of DGSS tasks remains rarely explored. The recent-developed Rein shows that fine-tuning VFM [10, 29] with learnable tokens yields the better generalization than the one with full parameter tuning [60].

2.3 Domain Generalized Semantic Segmentation

Semantic segmentation in driving scenes can encounter great domain shift, caused by factors such as adverse weather, diverse illumination, and urban landscape diversity [2, 25–27]. Domain adaptation methods [48, 69] have shown great successes, but they can only generalize to the target domain that has learned in the training stage. To generalize to arbitrary unseen target domains, DGSS has drawn increasing attentions in the past few years.

In the convolutional neural network (CNN) era, DGSS methods can be categorized into two types, namely style decoupling and style augmentation. For style-decoupling-based methods, instance normalization (e.g., IBN [42], Iternorm [23]) and instance whitening (e.g., IW [43], SAW [45], ISW [14], DIRM [61]) operations are commonly used. For style-augmentation-based methods, external training images from other sources are usually used to enrich the domain diversity [24, 33, 46, 66, 70, 72]. Later in the Vision Transformer (ViT) era, DGSS methods usually leverage the strong content representation ability of mask attention mechanism [3, 4, 18], which

learns a more global-wise representation than convolution and is more robust to the cross-domain style variation.

Nevertheless, the exploration of DGSS methods based on VFMs remains relatively limited. A recent work Rein shows that, fine-tuning VFM with learnable tokens yields better generalization for DGSS than full parameter tuning [60].

3 Methodology

The overview of the proposed Spectral-dEcomposed Tokens (SET) framework is shown in Fig. 3. To efficiently fine-tune VFMs, spectral-decomposed tokens are applied to each frozen layer. Within each layer, the frozen features are decomposed into amplitude and phase components by Fast Fourier Transform (FFT) (in Sec. 3.1). Spectral tokens are linked to amplitude and phase branches to extract the task-specific information and enhance the original features (in Sec. 3.2). Additionally, since the style variation mainly affects the amplitude component, we further design an attention optimization method to improve the generalization ability of the learned tokens (in Sec. 3.4). Finally, two enhanced components are projected back to the spatial space by Inverse Fast Fourier Transform (IFFT) and fed into the subsequent layer.

3.1 Spectral Decomposition

As discussed above, the low-frequency and high-frequency components in the frequency space provide a feasible solution to separate the content and style information. Inspired by this, we turn to the spectral decomposition [7, 44] via Fast Fourier Transform (FFT) to realize this objective. Specifically, given the intermediate image features $X_k \in \mathbb{R}^{d \times H \times W}$ of layer k , it is fed to a 2D Fast Fourier Transform, independent to each channel to obtain the corresponding projected representations $X_f \in \mathbb{R}^{d \times H \times W}$ in frequency space. This process on X_i within each channel can be computed as

$$X_f(x, y) = \sum_{h=0}^{H-1} \sum_{w=0}^{W-1} X_i(h, w) e^{-2j\pi(x\frac{h}{H} + y\frac{w}{W})}, \quad (1)$$

where H and W are the height and the width of the image features. In addition, d denotes the feature dimension.

On the other hand, the inverse transformation from the frequency space to the spatial space is usually implemented by the Inverse Fast Fourier Transform (IFFT), which is mathematically computed as

$$X_k(h, w) = \frac{1}{HW} \sum_{x=0}^{H-1} \sum_{y=0}^{W-1} X_f(x, y) e^{2j\pi(x\frac{h}{H} + y\frac{w}{W})}. \quad (2)$$

The frequency representation X_f can be divided into two parts, namely the real part X_f^{real} and the imagery part X_f^{img} respectively, defined as

$$X_f(x, y) = X_f^{real} + iX_f^{img}. \quad (3)$$

Decomposing the image feature X_i into its amplitude α and phase ρ is known as spectral decomposition, given by

$$\alpha = \sqrt{(X_f^{real})^2 + (X_f^{img})^2}, \quad \rho = \arctan(X_f^{img}/X_f^{real}). \quad (4)$$

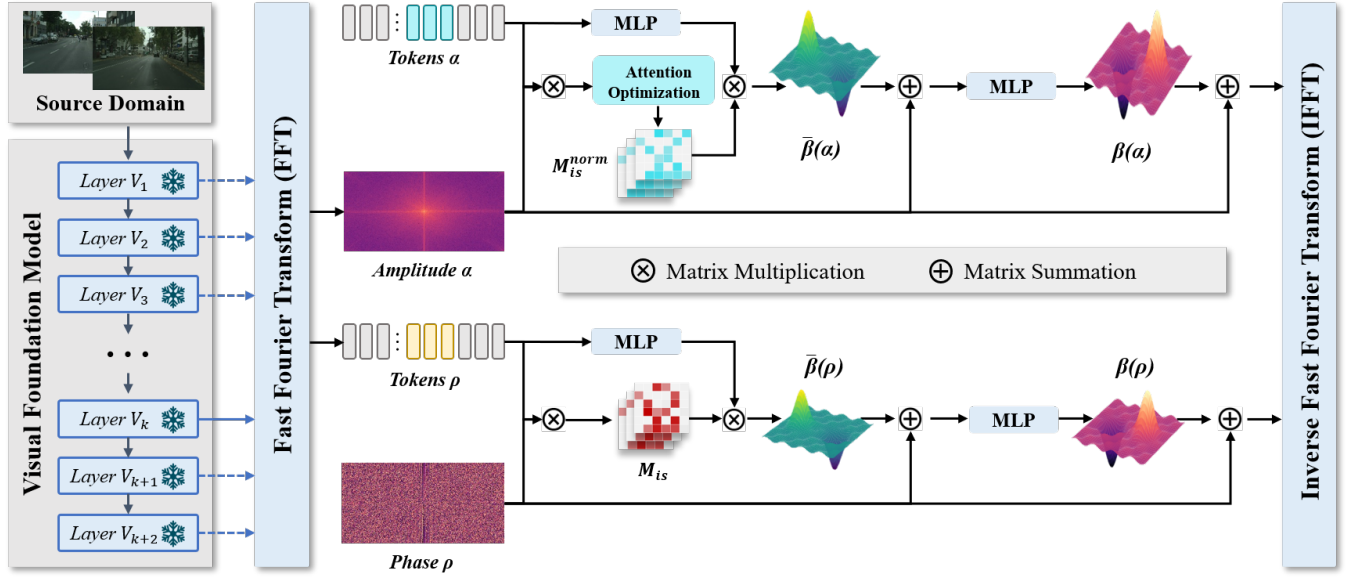


Figure 3: Framework overview of the proposed Spectral-decomposed Token (SET) learning scheme. Embedded into each frozen layer of a VFM, the proposed SET consists of three steps, namely spectral decomposition (in Sec. 3.1), learning spectral tokens (in Sec. 3.2) and attention optimization in amplitude branch (in Sec. 3.3). By default, DINOv2 [40] is used as the frozen VFM, while the proposed SET is versatile to different VFMs.

Through this series of mathematical transformations, the frequency representation X_f can be presented as

$$X_f = \alpha \cos(\rho) + i \alpha \sin(\rho). \quad (5)$$

Define the function to decompose the frequency feature into its amplitude and phase components as $decompose(\cdot)$, and the opposite process as $compose(\cdot)$, this process can be presented as

$$\alpha, \rho = decompose(X_k), \quad X_k = compose(\alpha, \rho). \quad (6)$$

3.2 Learning Spectral Tokens

Leveraging learnable tokens with only a few number of parameters [21] has been turned out to be an effective path to fine-tune the VFMs. Following this simple yet effective paradigm, in our pipeline, learnable tokens are utilized to refine the spectral components α_k and ρ_k of features at each layer within the frozen VFM backbone. Since these tokens refine the original features in the frequency domain, we name them as spectral tokens in this paper. Specifically, for the features X_k generated by the k -th layer V_k , spectral components α_k, ρ_k is obtained by spectral decomposition. The enhanced spectral features $\hat{\alpha}_k, \hat{\rho}_k$ are produced by token-based adjustment $\beta(\cdot)$ and composed to output feature as the input for the subsequent layer, given by

$$\alpha_k, \rho_k = decompose(X_k), \hat{\alpha}_k = \alpha_k + \beta(\alpha_k), \hat{\rho}_k = \rho_k + \beta(\rho_k), \quad (7)$$

$$X_{k+1} = V_{k+1}(compose(\hat{\alpha}_k, \hat{\rho}_k)).$$

Assume we have a set of spectral tokens $T = \{T_i^D \in \mathbb{R}^{l \times d} | D \in [\alpha, \rho], 1 \leq i \leq N\}$, where T_k^α and T_k^ρ denote the learnable tokens

for α_k and ρ_k , respectively. N is the number of layers in VFM, l denote the length of each token (number of features in each token), and d denote the feature dimension of T_i , which is equal to the channel number in spectral-decomposed features. During training, the backbone is kept frozen and the task-specific posterior is acquired from the DGSS dataset through these spectral tokens, bridging the scene disparity concerning the pre-training datasets and fine-tuning datasets.

To achieve this, each spectral token includes a bag of learnable features to capture the task-specific knowledge in frequency domain. Within the token-based adjustment process $\beta(\cdot)$, these bag features are used to enhance the spectral-decomposed features based on their similarity. Through this enhancement, task-relevant representations in the original features are further highlighted, while task-irrelevant category information is partially filtered out.

Specifically, inner-product is utilized to measure the similarity between token features and original features from frozen layers. Similarity map $M_k^\alpha \in \mathbb{R}^{HW \times l}$ is built to capture the association between spectral-decomposed features (α_k as example) and spectral token (amplitude token T_k^α as example). Following the widely-used attention mechanism, a softmax function is applied to each line of M_k^α to normalize the weights of token features. To summarize, the feature-token similarity can be mathematically computed as

$$M_k^\alpha = Softmax\left(\frac{\alpha_k \times T_k^\alpha}{\sqrt{d}}\right). \quad (8)$$

Through the feature-token similarity map M_k^α , we can select the relevant token features for each position of the spectral-decomposed features. These relevant token features include learned task-specific knowledge which is used to enhance the original features. Before added into the frozen spectral-decomposed features, the token features are further processed by a Multi-Layer Perceptron (MLP) layer to generate a more suitable representation for enhancement. This intermediate process $\bar{\beta}(\alpha_k)$ can be presented as

$$\bar{\beta}(\alpha_k) = M_k^\alpha \times MLP(T_k^\alpha). \quad (9)$$

Finally, another MLP layer is adapted to the enhanced features. This layer is designed to extract task-related information and filter out the irrelevant representations. The overall process of token-based adjustment $\beta(\cdot)$ can be written as

$$\beta(\alpha_k) = MLP(\alpha_k + \bar{\beta}(\alpha_k)), \quad \beta(\rho_k) = MLP(\rho_k + \bar{\beta}(\rho_k)). \quad (10)$$

3.3 Attention Optimization

During inference, the parameters of the learnable tokens are fixed. As shown in Fig. 2, the style variations can significantly reflect in the amplitude component. As a result, when dealing with images from unseen target domains, the weights of the feature-token similarity map in the amplitude branch may be severely affected by the style change. Since the task-related category information is stored in the tokens features, the perturbation of weights leads to the injection of incorrect category information during the enhancement process, thereby weakening the domain generalization ability. To address this problem, we further proposed an attention optimization method to adjust the similarity map in amplitude branch.

Specifically, we perform a further normalization on the feature-token similarity map,

$$M_k^{norm} = \frac{M_k^\alpha - \mu}{\sigma}, \quad (11)$$

where μ and σ denote the mean and standard deviation of M_k^α . Let H, W denote the size of similarity map, μ and σ are computed by

$$\mu = \frac{1}{HW} \sum_{i=1}^H \sum_{j=1}^W M_{i,j}, \quad \sigma^2 = \frac{1}{HW} \sum_{i=1}^H \sum_{j=1}^W (M_{i,j} - \mu)^2. \quad (12)$$

Due to the softmax operation when acquiring M_k^α , the original mean value of M_k^α is $\frac{1}{l}$ and the max standard deviation is $\sqrt{\frac{1}{l}(1 - \frac{1}{l})}$, where l is the number of features in each token. After normalization, the standard deviation increases to 1, which means higher weights are assigned to the relevant token features and the weight distribution becomes more uneven. When amplitude feature representation affected by style variation, its similarity with fixed tokens trained on source dataset decreases, leading to more uniform weight distribution within the feature-token similarity map. By the proposed attention optimization, the weight distribution is refined and the relevant token features receive more attention, alleviating the impacts of style change for token-based fine-tuning. After that, the enhancement process in amplitude branch can be written as

$$\hat{\alpha}_k^{norm} = \alpha_k + MLP(\alpha_k + M_k^{norm} \times MLP(T_k^\alpha)). \quad (13)$$

Finally, amplitude component is combined with phase component, projected back to the spatial space and fed into the next layer

in VFM, given by

$$X_{k+1} = V_{k+1}(\text{compose}(\hat{\alpha}_k^{norm}, \hat{\rho}_k)). \quad (14)$$

3.4 Implementation Details

Following prior work [60], the model is trained 40000 iterations with a batch size of 4 and an initial learning rate of 1e-4 for DGSS tasks. The resolution of input images is 512×512. DINOv2 is chosen as the default VFM, and the segmentation head of Mask2Former [13] is utilized to produce pixel-level prediction.

4 Experiment

4.1 Datasets & Evaluation Protocols

4.1.1 Datasets. We conduct the experiments on five driving-scene semantic segmentation datasets.

CityScapes [16] is constructed based on the driving-scenes in Germany cities, which includes 2,975 and 500 well-annotated samples for training and validation, respectively. The resolution of CityScapes is 2,048×1,024.

BDD-100K [65] provides diverse scenes of driving videos under various weather conditions. It contains 7,000 and 1,000 fine-annotated samples for training and validation of semantic segmentation, respectively. The resolution of BDD-100K is of 1,280×720.

SYNTHIA [53] provides a large-scale synthetic dataset, and provides 9,400 images with a resolution of 1,280×760.

Mapillary [38] provides a large-scale semantic segmentation dataset based on street scenes with 25,000 samples.

GTAV [52] is a synthetic semantic segmentation dataset rendered by the GTAV game engine. It provides 24,966 simulated urban-street samples with a resolution of 1,914×1,052.

4.1.2 Evaluation Settings. We illustrate our domain generalization settings as follows. Firstly, we use C, B, S, M and G to denote the above five datasets respectively. Following prior DGSS works [14, 42, 43, 45], the segmentation model is trained on one dataset as the **source domain**, and is validated on the rest of the four datasets as the **target domains**. Three settings include: 1) $G \rightarrow \{C, B, M, S\}$; 2) $S \rightarrow \{C, B, M, G\}$; and 3) $C \rightarrow \{B, M, G, S\}$. We employ the mIoU (%) metric for the evaluation. All the reported performance is directly cited from prior works [14, 42, 43, 45].

4.1.3 Baselines. Existing DGSS methods are included for comparison, namely, IBN [42], IW [43], Iternorm [23], DRPC [66], ISW [14], GTR [46], DURL [61], SHADE [70], SAW [45], WildNet [33], AdvStyle [72], SPC [24], HGFormer [18], CMFormer [3], DINDEX [39] and Rein [60].

4.2 Comparison with State-of-the-art

4.2.1 GTAV Source Domain. Table 1 compares the performance of the proposed SET with existing state-of-the-art DGSS methods under the $G \rightarrow \{C, B, M, S\}$ setting. The proposed SET shows an mIoU improvement of 1.66%, 1.24%, 1.58% and 1.15% on C, B, M and S unseen target domains, respectively, compared to the VFM based state-of-the-art Rein [60]. In addition, the mIoU improvements on ResNet based and Mask2Former based DGSS methods are more than 20% and 10%, respectively. It is worthy noting that the source

Table 1: $G \rightarrow \{C, B, M, S\}$ setting. Performance comparison between the proposed SET (ours) and existing DGSS methods. '-': The metric is either not reported or the official source code is not available. Evaluation metric mIoU is given in (%). '': only one decimal result is reported. '+': results are re-implemented.**

Method	Venue	Trained on GTAV (G)			
		→ C	→ B	→ M	→ S
<i>ResNet based:</i>					
IBN [42]	ECCV 2018	33.85	32.30	37.75	27.90
IW [43]	CVPR 2019	29.91	27.48	29.71	27.61
Itemnorm [23]	CVPR 2019	31.81	32.70	33.88	27.07
DRPC [66]	ICCV 2019	37.42	32.14	34.12	28.06
ISW [14]	CVPR 2021	36.58	35.20	40.33	28.30
GTR [46]	TIP 2021	37.53	33.75	34.52	28.17
DIRL [61]	AAAI 2022	41.04	39.15	41.60	-
SHADE [70]	ECCV 2022	44.65	39.28	43.34	-
SAW [45]	CVPR 2022	39.75	37.34	41.86	30.79
WildNet [33]	CVPR 2022	44.62	38.42	46.09	31.34
AdvStyle [72]	NeurIPS 2022	39.62	35.54	37.00	-
SPC [24]	CVPR 2023	44.10	40.46	45.51	-
<i>Mask2Former based:</i>					
CMFormer [3]	AAAI 2024	55.31	49.91	60.09	43.80
<i>VFM based:</i>					
DIDEX* [39]	WACV 2024	62.0	54.3	63.0	-
REIN* [60]	CVPR 2024	66.4	60.4	66.1	48.86 [†]
Ours	MM 2024	68.06	61.64	67.68	50.01
		↑1.66	↑1.24	↑1.58	↑1.15

Table 2: $S \rightarrow \{C, B, M, G\}$ setting. Performance comparison between the proposed SET (ours) and existing DGSS methods. '-': The metric is either not reported or the official source code is not available. Evaluation metric mIoU is given in (%). '': only one decimal result is reported. '+': results are re-implemented.**

Method	Venue	Trained on SYNTHIA (S)			
		→ C	→ B	→ M	→ G
<i>ResNet based:</i>					
IBN [42]	ECCV 2018	32.04	30.57	32.16	26.90
IW [43]	CVPR 2019	28.16	27.12	26.31	26.51
DRPC [66]	ICCV 2019	35.65	31.53	32.74	28.75
ISW [14]	CVPR 2021	35.83	31.62	30.84	27.68
GTR [46]	TIP 2021	36.84	32.02	32.89	28.02
SAW [45]	CVPR 2022	38.92	35.24	34.52	29.16
AdvStyle [72]	NeurIPS 2022	37.59	27.45	31.76	-
<i>Mask2Former based:</i>					
CMFormer [3]	AAAI 2024	44.59	33.44	43.25	40.65
<i>VFM based:</i>					
REIN [†] [60]	CVPR 2024	48.59	44.42	48.64	46.97
Ours	MM 2024	49.65	45.45	49.45	48.05
		↑1.06	↑1.03	↑0.81	↑1.08

domain GTAV is a synthetic dataset, while C, B and M target domains are real datasets. The positive outcomes under this setting demonstrates the feature generalization ability of the proposed SET.

4.2.2 SYNTHIA Source Domain. Table 2 compares the performance of the proposed SET and existing state-of-the-art DGSS methods

Table 3: $C \rightarrow \{B, M, G, S\}$ setting. Performance comparison between the proposed SET (ours) and existing DGSS methods. '-': the metric is either not reported or the official source code is not available. Evaluation metric mIoU is given in (%). '+': results are re-implemented.

Method	Venue	Trained on Cityscapes (C)			
		→ B	→ M	→ G	→ S
<i>ResNet based:</i>					
IBN [42]	ECCV 2018	48.56	57.04	45.06	26.14
IW [43]	CVPR 2019	48.49	55.82	44.87	26.10
Iternorm [23]	CVPR 2019	49.23	56.26	45.73	25.98
DRPC [66]	ICCV 2019	49.86	56.34	45.62	26.58
ISW [14]	CVPR 2021	50.73	58.64	45.00	26.20
GTR [46]	TIP 2021	50.75	57.16	45.79	26.47
DIRL [61]	AAAI 2022	51.80	-	46.52	26.50
SHADE [70]	ECCV 2022	50.95	60.67	48.61	27.62
SAW [45]	CVPR 2022	52.95	59.81	47.28	28.32
WildNet [33]	CVPR 2022	50.94	58.79	47.01	27.95
<i>Mask2Former based:</i>					
HGFormer* [18]	CVPR 2023	53.4	66.9	51.3	33.6
CMFormer [3]	AAAI 2024	59.27	71.10	58.11	40.43
<i>VFM based:</i>					
REIN [†] [60]	CVPR 2024	63.54	74.03	62.41	48.56
Ours	MM 2024	65.07	75.67	63.80	49.61
		↑1.53	↑1.64	↑1.39	↑1.05

Table 4: Ablation studies on key components of SET under the $G \rightarrow \{C, B, M, S\}$ setting. VFM: use only frozen VFM to predict, Spe.: spectral decomposition, Token: spectral tokens, AO: attention optimization.

Component				Trained on GTAV (G)			
VFM	Spe.	Token	AO	$\rightarrow C$	$\rightarrow B$	$\rightarrow M$	$\rightarrow S$
✓				63.30	56.10	63.90	46.50
✓	✓			65.23	59.34	64.32	47.10
✓		✓		66.40	60.40	66.10	48.86
✓	✓	✓		66.78	60.59	66.08	48.92
✓	✓	✓	✓	68.06	61.64	67.68	50.01

under the $S \rightarrow \{C, B, M, G\}$ setting. The proposed SET shows improvements of 1.06%, 1.03%, 0.81% and 1.08% on mIoU against the runner-up method Rein [60]. In addition, the mIoU improvements on ResNet based and Mask2Former based DGSS methods are more than 20% and 10%, respectively, when generalized to B, M and G unseen target domains.

4.2.3 CityScapes Source Domain. Table 3 compares the performance of the proposed SET and existing state-of-the-art DGSS methods under the $C \rightarrow \{B, M, G, S\}$ setting. The proposed SET also shows a clear performance improvement than the second-best Rein [60]. Specifically, the mIoU improvements on the B, M, G and S unseen target domains are 1.53%, 1.64%, 1.39% and 1.05%, respectively. In addition, the mIoU improvements on ResNet based and Mask2Former based DGSS methods are more than 15% and 8% in average. To better understand how the proposed SET improves the

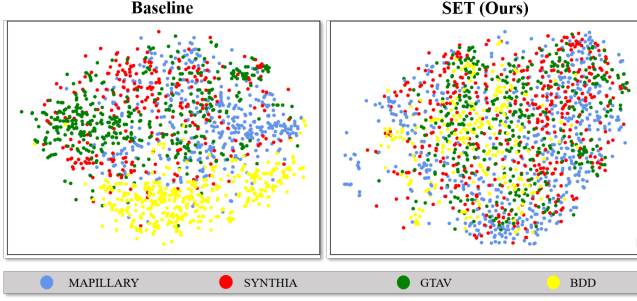


Figure 4: T-SNE visualization of the feature space from baseline (left), and the proposed SET (RDWT; right). The model is trained on the CityScapes source domain, and inferred on the rest four unseen target domains. The proposed SET allows the unseen target domain samples to be more uniformly distributed. Better zoom in to view.

Table 5: Ablation studies on attention optimization within different components. *Image* denotes the original image features, *Phase* denotes phase component, *Amplitude* denotes amplitude component.

Attention Optimization			Trained on GTAV (G)			
Image	Phase	Amplitude	→ C	→ B	→ M	→ S
✓			64.91	56.97	64.20	46.72
	✓		63.27	56.38	62.71	46.08
	✓	✓	66.01	58.83	64.62	48.16
		✓	68.06	61.64	67.68	50.01

feature generalization when compared with Rein [60], Fig. 4 visualizes the feature space of the Rein baseline (left) and the proposed SET (right). The proposed SET allows the samples from different unseen target domains to be more uniformly distributed.

4.3 Ablation Studies

4.3.1 On Key Components. Table 4 studies the impact of each component in the proposed SET. The experiments are conducted under the $G \rightarrow \{C, B, M, S\}$ setting. When only the frozen VFM (DINOv2) is used for DGSS (in the first row), the mIoU is relatively low. The spectral decomposition operation (in the second row) contributes to 1.93%, 3.24%, 0.42% and 0.60% mIoU gain on the C, B, M and S target domains by separately learning the amplitude and phase information. Furthermore, when spectral tokens are implemented (in the third row), the performance gain are 3.10%, 4.30%, 3.10% and 2.36% mIoU on the C, B, M and S target domains, respectively. Finally, based on the spectral tokens, attention optimization contributes to an additional improvement of 1.28%, 1.05%, 1.60% and 1.09%.

4.3.2 On Attention Optimization. Table 5 further studies the attention optimization operation on each component. The outcomes show that, attention optimization in phase branch can potentially harm the model’s representational capability. In contrast, the optimal choice is to only use for amplitude component, which shows the most predominate improvement on the generalization ability.

Table 6: Generalization ability test of the proposed SET on different VFM models. One decimal result is reported and compared following prior references.

Backbone	Fine-tune Method	Trainable Params*	mIoU			
			Citys	BDD	Map	Avg.
CLIP [50]	Full	304.15M	51.3	47.6	54.3	51.1
	Freeze	0.00M	53.7	48.7	55.0	52.4
	Rein [60]	2.99M	57.1	54.7	60.5	57.4
	SET	6.13M	58.2	55.3	61.4	58.3
MAE [20]	Full	330.94M	53.7	50.8	58.1	54.2
	Freeze	0.00M	43.3	37.8	48.0	43.0
	Rein [60]	2.99M	55.0	49.3	58.6	54.3
	SET	6.13M	56.2	51.0	60.2	55.8
SAM [31]	Full	632.18M	57.6	51.7	61.5	56.9
	Freeze	0.00M	57.0	47.1	58.4	54.2
	Rein [60]	4.51M	59.6	52.0	62.1	57.9
	SET	9.21M	60.7	52.8	63.2	58.9
EVA02 [19]	Full	304.24M	62.1	56.2	64.6	60.9
	Freeze	0.00M	56.5	53.6	58.6	56.2
	Rein [60]	2.99M	65.3	60.5	64.9	63.6
	SET	6.13M	66.4	61.8	65.6	64.6
DINOv2 [40]	Full	304.20M	63.7	57.4	64.2	61.7
	Freeze	0.00M	63.3	56.1	63.9	61.1
	Rein [60]	2.99M	66.4	60.4	66.1	64.3
	SET	6.13M	68.0	61.6	67.6	65.7

Table 7: Generalization of the proposed CMFormer to the adverse condition domains (rain, fog, night and snow) on ACDC dataset [54]. ‘*’: Only reports one decimal results. ‘†’: Reports re-implementation result.

Method	Venue	Trained on Cityscapes (C)			
		→ Fog	→ Night	→ Rain	→ Snow
<i>ResNet based:</i>					
IBN* [42]	ECCV 2018	63.8	21.2	50.4	49.6
IW* [43]	CVPR 2019	62.4	21.8	52.4	47.6
ISW* [14]	CVPR 2021	64.3	24.3	56.0	49.8
<i>Mask2Former based:</i>					
ISSA* [34]	WACV 2023	67.5	33.2	55.9	53.2
CMFormer* [3]	AAAI 2024	77.8	33.7	67.6	64.3
<i>VFM based:</i>					
Rein [†] [60]	CVPR 2024	79.48	55.92	72.45	70.57
Ours	MM 2024	80.06	57.29	74.80	73.69
		↑0.58	↑1.37	↑2.35	↑3.12

4.4 Generalization Ability Test

4.4.1 On Different VFMs. We validate if the proposed SET can be generalized to a variety of VFMs. It is integrated into CLIP [50], MAE [20], SAM [31], EVA02 [19] and DINOv2 [40] under full-training, full-freezing and fine-tuning scheme, respectively. One decimal result is reported and compared following prior references. Besides, Rein [60], as the fine-tuning baseline, is also involved for comparison. Table 6 reports the outcomes under the $G \rightarrow \{C, B, M\}$ setting. Our SET shows a significant performance improvement than Rein [60] and other methods with all listed VFMs.

4.4.2 On Adverse Conditions. Adverse Conditions Dataset with Correspondences (ACDC) (ACDC) [54] is the largest semantic segmentation dataset under adverse conditions. Following prior works, fog, night, rain and snow are set as four different unseen domains.

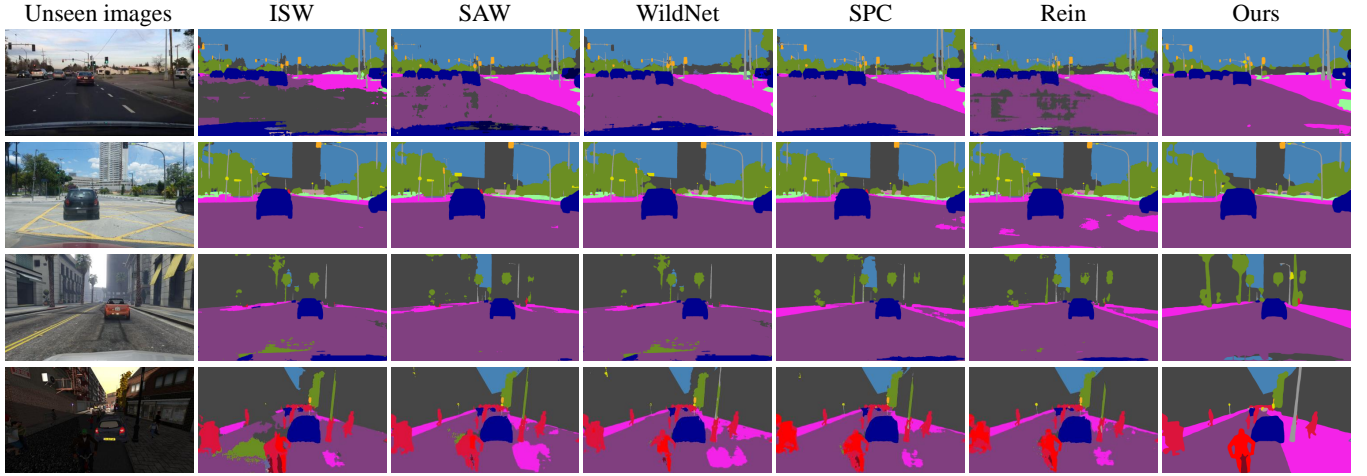


Figure 5: Visual segmentation results on unseen target domains under the $C \rightarrow B, M, G, S$ setting. The proposed SET is compared with ISW [14], SAW [45], WildNet [33], SPC [24] and Rein [60].

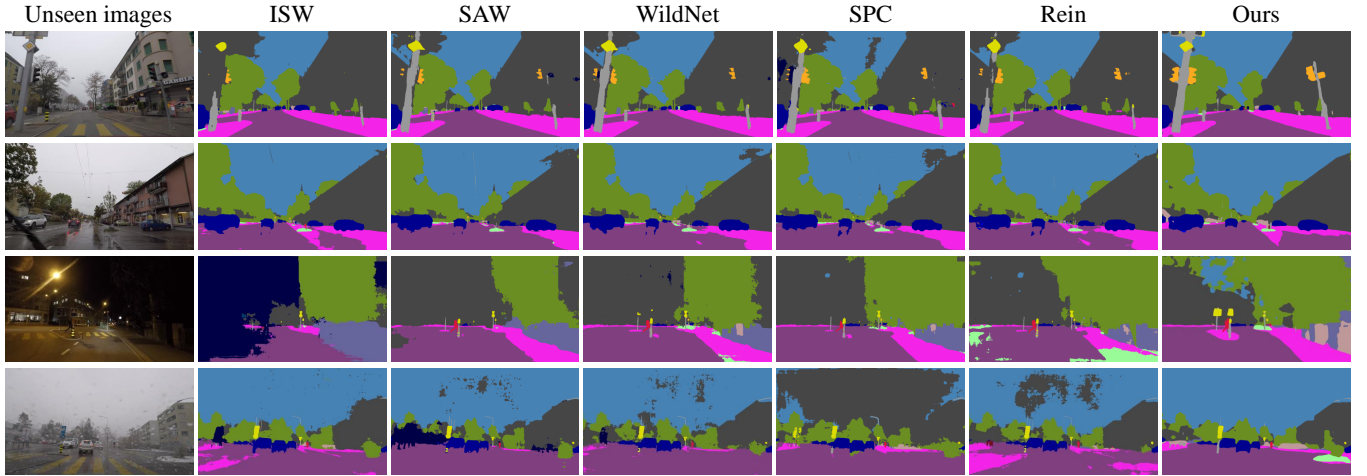


Figure 6: Visual segmentation results on unseen target domains under the $C \rightarrow ACDC$ setting. The proposed SET is compared with ISW [14], SAW [45], WildNet [33], SPC [24] and Rein [60].

CityScapes is used as the source domain. Table 7 compares the performance between SET and existing methods. It significantly outperforms existing ResNet based methods by at least 20% mIoU and Mask2Former based methods by at least 10% mIoU on all the adverse domains. Notably, compared with Rein [60] baseline, our SET shows improvements of 0.58%, 1.37%, 2.35% and 3.12% on mIoU in the fog, night, rain and snow domain, respectively.

4.5 Quantitative Segmentation Results

Fig. 5 demonstrates some visual segmentation results on unseen target domains under the $C \rightarrow B, M, G, S$ setting. Fig. 6 illustrates the visual segmentation results under the $C \rightarrow ACDC$ setting. On both settings, the segmentation results show that the proposed SET shows better pixel-wise prediction than the compared DGSS methods, especially in terms of the completeness of objects.

5 Conclusion

In this paper, we aim to fine-tune VFM for the down-stream task DGSS. While the VFMs have inherent generalization to out-of-distribution, how to exploit the style-invariant property of a VFM remains to be the bottleneck. We propose a Spectral-Decomposed Token (SET) learning scheme. As the content and style information in a scene reflects more from the low- and high- frequency components in the frequency space, we transform the frozen VFM features into the phase and amplitude components respectively. Then, spectral tokens are adapted to enhance the learning of task-specific knowledge within each branch. As the cross-domain differences mainly affects the amplitude branch, an attention optimization method is further proposed to mitigate the impacts of style variation. Extensive experiments under multiple cross-domain settings show the state-of-the-art performance of the proposed SET and its flexibility on a variety of VFMs.

References

- [1] Qi Bi, Jingjun Yi, Hao Zheng, Wei Ji, Yawen Huang, Yuexiang Li, and Yefeng Zheng. 2024. Learning Generalized Medical Image Segmentation from Decoupled Feature Queries. In *Proceedings of the AAAI Conference on Artificial Intelligence*, Vol. 38. 810–818.
- [2] Qi Bi, Shaodi You, and Theo Gevers. 2023. Interactive Learning of Intrinsic and Extrinsic Properties for All-Day Semantic Segmentation. *IEEE Transactions on Image Processing* 32 (2023), 3821–3835.
- [3] Qi Bi, Shaodi You, and Theo Gevers. 2024. Learning Content-Enhanced Mask Transformer for Domain Generalized Urban-Scene Segmentation. In *Proceedings of the AAAI Conference on Artificial Intelligence*, Vol. 38. 819–827.
- [4] Qi Bi, Shaodi You, and Theo Gevers. 2024. Learning Generalized Segmentation for Foggy-Scenes by Bi-directional Wavelet Guidance. In *Proceedings of the AAAI Conference on Artificial Intelligence*, Vol. 38. 801–809.
- [5] E Oran Brigham. 1988. *The Fast Fourier Transform and Its Applications*. Prentice-Hall, Inc.
- [6] Silvia Bucci, Antonio D’Innocente, Yujun Liao, Fabio M Carlucci, Barbara Caputo, and Tatiana Tommasi. 2021. Self-supervised learning across domains. *IEEE Transactions on Pattern Analysis and Machine Intelligence* 44, 9 (2021), 5516–5528.
- [7] John P Castagna and Shengjie Sun. 2006. Comparison of Spectral Decomposition Methods. *First break* 24, 3 (2006).
- [8] Guangyao Chen, Peixi Peng, Li Ma, Jia Li, Lin Du, and Yonghong Tian. 2021. Amplitude-Phase Recombination: Rethinking Robustness of Convolutional Neural Networks in Frequency Domain. In *Proceedings of the IEEE/CVF International Conference on Computer Vision*. 458–467.
- [9] Jin Chen, Zhi Gao, Xinxiao Wu, and Jiebo Luo. 2023. Meta-Causal Learning for Single Domain Generalization. In *Proceedings of the IEEE/CVF Conference on Computer Vision and Pattern Recognition*. 7683–7692.
- [10] Shoufa Chen, Chongjian Ge, Zhan Tong, Jiangliu Wang, Yibing Song, Jue Wang, and Ping Luo. 2022. Adaptformer: Adapting Vision Transformers for Scalable Visual Recognition. *Advances in Neural Information Processing Systems* 35 (2022), 16664–16678.
- [11] Sentao Chen, Lei Wang, Zijie Hong, and Xiaowei Yang. 2023. Domain Generalization by Joint-Product Distribution Alignment. *Pattern Recognition* 134 (2023), 109086.
- [12] Wei-Ting Chen, Zhi-Kai Huang, Cheng-Che Tsai, Hao-Hsiang Yang, Jian-Jiun Ding, and Sy-Yen Kuo. 2022. Learning Multiple Adverse Weather Removal via Two-Stage Knowledge Learning and Multi-Contrastive Regularization: Toward a Unified Model. In *Proceedings of the IEEE/CVF Conference on Computer Vision and Pattern Recognition*. 17653–17662.
- [13] Bowen Cheng, Ishan Misra, Alexander G Schwing, Alexander Kirillov, and Rohit Girdhar. 2022. Masked-Attention Mask Transformer for Universal Image Segmentation. In *Proceedings of the IEEE/CVF Conference on Computer Vision and Pattern Recognition*. 1290–1299.
- [14] Sungha Choi, Sanghun Jung, Huiwon Yun, Joanne T Kim, Seungryong Kim, and Jaegul Choo. 2021. Robustnet: Improving Domain Generalization in Urban-Scene Segmentation via Instance Selective Whitening. In *Proceedings of the IEEE/CVF Conference on Computer Vision and Pattern Recognition*. 11580–11590.
- [15] Seokeon Choi, Taekyung Kim, Minki Jeong, Hyoungseob Park, and Changick Kim. 2021. Meta Batch-Instance Normalization for Generalizable Person Re-Identification. In *Proceedings of the IEEE/CVF conference on Computer Vision and Pattern Recognition*. 3425–3435.
- [16] Marius Cordts, Mohamed Omran, Sebastian Ramos, Timo Rehfeld, Markus Enzweiler, Rodrigo Benenson, Uwe Franke, Stefan Roth, and Bernt Schiele. 2016. The Cityscapes Dataset for Semantic Urban Scene Understanding. In *Proceedings of the IEEE Conference on Computer Vision and Pattern Recognition*. 3213–3223.
- [17] Aveen Dayal, Vimal KB, Linga Reddy Cenkeramaddi, C Mohan, Abhinav Kumar, and Vineeth N Balasubramanian. 2024. MADG: Margin-based Adversarial Learning for Domain Generalization. *Advances in Neural Information Processing Systems* 36 (2024).
- [18] Jian Ding, Nan Xue, Gui-Song Xia, Bernt Schiele, and Dengxin Dai. 2023. HGFormer: Hierarchical Grouping Transformer for Domain Generalized Semantic Segmentation. In *Proceedings of the IEEE/CVF Conference on Computer Vision and Pattern Recognition*. 15413–15423.
- [19] Yuxin Fang, Wen Wang, Binhui Xie, Quan Sun, Ledell Wu, Xinggang Wang, Tiejun Huang, Xinlong Wang, and Yue Cao. 2023. Eva: Exploring the Limits of Masked Visual Representation Learning at Scale. In *Proceedings of the IEEE/CVF Conference on Computer Vision and Pattern Recognition*. 19358–19369.
- [20] Kaiming He, Xinlei Chen, Saining Xie, Yanghao Li, Piotr Dollár, and Ross Girshick. 2022. Masked Autoencoders are Scalable Vision Learners. In *Proceedings of the IEEE/CVF Conference on Computer Vision and Pattern Recognition*. 16000–16009.
- [21] Edward J Hu, Yelong Shen, Phillip Wallis, Zeyuan Allen-Zhu, Yuanzhi Li, Shean Wang, Lu Wang, and Weizhu Chen. 2021. Lora: Low-Rank Adaptation of Large Language Models. *arXiv preprint arXiv:2106.09685* (2021).
- [22] Jiaxing Huang, Dayan Guan, Aoran Xiao, and Shijian Lu. 2021. Fsd: Frequency space domain randomization for domain generalization. In *Proceedings of the IEEE/CVF conference on computer vision and pattern recognition*. 6891–6902.
- [23] Lei Huang, Yi Zhou, Fan Zhu, Li Liu, and Ling Shao. 2019. Iterative Normalization: Beyond Standardization towards Efficient Whitening. In *Proceedings of the IEEE/CVF Conference on Computer Vision and Pattern Recognition*. 4874–4883.
- [24] Wei Huang, Chang Chen, Yong Li, Jiacheng Li, Cheng Li, Fenglong Song, Youliang Yan, and Zhiwei Xiong. 2023. Style Projected Clustering for Domain Generalized Semantic Segmentation. In *Proceedings of the IEEE/CVF Conference on Computer Vision and Pattern Recognition*. 3061–3071.
- [25] Wei Ji, Jingjing Li, Qi Bi, Tingwei Liu, Wenbo Li, and Li Cheng. 2024. Segment Anything Is Not Always Perfect: An Investigation of SAM on Different Real-world Applications. *Machine Intelligence Research* 21 (2024), 617–630.
- [26] Wei Ji, Jingjing Li, Cheng Bian, Zhicheng Zhang, and Li Cheng. 2023. Semanti-RT: A Large-Scale Dataset and Method for Robust Semantic Segmentation in Multispectral Images. In *Proceedings of the 31st ACM International Conference on Multimedia*. 3307–3316.
- [27] Wei Ji, Jingjing Li, Cheng Bian, Zongwei Zhou, Jiaying Zhao, Alan L Yuille, and Li Cheng. 2023. Multispectral Video Semantic Segmentation: A Benchmark Dataset and Baseline. In *Proceedings of the IEEE/CVF Conference on Computer Vision and Pattern Recognition*. 1094–1104.
- [28] Wei Ji, Shuang Yu, Junde Wu, Kai Ma, Cheng Bian, Qi Bi, Jingjing Li, Hanruo Liu, Li Cheng, and Yefeng Zheng. 2021. Learning calibrated medical image segmentation via multi-rater agreement modeling. In *Proceedings of the IEEE/CVF Conference on Computer Vision and Pattern Recognition*. 12341–12351.
- [29] Menglin Jia, Luming Tang, Bor-Chun Chen, Claire Cardie, Serge Belongie, Bharath Hariharan, and Ser-Nam Lim. 2022. Visual Prompt Tuning. In *European Conference on Computer Vision*. Springer, 709–727.
- [30] Daehee Kim, Youngjun Yoo, Seunghyun Park, Jinkyu Kim, and Jaekoo Lee. 2021. Selfreg: Self-Supervised Contrastive Regularization for Domain Generalization. In *Proceedings of the IEEE/CVF International Conference on Computer Vision*. 9619–9628.
- [31] Alexander Kirillov, Eric Mintun, Nikhila Ravi, Hanzi Mao, Chloe Rolland, Laura Gustafson, Tete Xiao, Spencer Whitehead, Alexander C Berg, Wan-Yen Lo, et al. 2023. Segment Anything. In *Proceedings of the IEEE/CVF International Conference on Computer Vision*. 4015–4026.
- [32] Sangrok Lee, Jongseong Bae, and Ha Young Kim. 2023. Decompose, Adjust, Compose: Effective Normalization by Playing with Frequency for Domain Generalization. In *Proceedings of the IEEE/CVF Conference on Computer Vision and Pattern Recognition*. 11776–11785.
- [33] Suhyeon Lee, Hongje Seong, Seongwon Lee, and Euntai Kim. 2022. WildNet: Learning Domain Generalized Semantic Segmentation from the Wild. In *Proceedings of the IEEE/CVF Conference on Computer Vision and Pattern Recognition*. 9936–9946.
- [34] Yumeng Li, Dan Zhang, Margret Keuper, and Anna Khoreva. 2023. Intra-Source Style Augmentation for Improved Domain Generalization. In *Proceedings of the IEEE/CVF Winter Conference on Applications of Computer Vision*. 509–519.
- [35] Yawei Luo, Ping Liu, Tao Guan, Junqing Yu, and Yi Yang. 2020. Adversarial style mining for one-shot unsupervised domain adaptation. *Advances in neural information processing systems* 33 (2020), 20612–20623.
- [36] M Jehanzeb Mirza, Marc Masana, Horst Possegger, and Horst Bischof. 2022. An Efficient Domain-Incremental Learning Approach to Drive in All Weather Conditions. In *Proceedings of the IEEE/CVF Conference on Computer Vision and Pattern Recognition*. 3001–3011.
- [37] Hyeonseob Nam and Hyo-Eun Kim. 2018. Batch-Instance Normalization for Adaptively Style-Invariant Neural Networks. *Advances in Neural Information Processing Systems* 31 (2018).
- [38] Gerhard Neuhold, Tobias Ollmann, Samuel Rota Buló, and Peter Kotschieder. 2017. The Mapillary Vistas Dataset for Semantic Understanding of Street Scenes. In *Proceedings of the IEEE International Conference on Computer Vision*. 4990–4999.
- [39] Joshua Niemeijer, Manuel Schwonberg, Jan-Aike Termöhlen, Nico M Schmidt, and Tim Fingscheidt. 2024. Generalization by Adaptation: Diffusion-Based Domain Extension for Domain-Generalized Semantic Segmentation. In *Proceedings of the IEEE/CVF Winter Conference on Applications of Computer Vision*. 2830–2840.
- [40] Maxime Oquab, Timothée Darcet, Théo Moutakanni, Huy Vo, Marc Szafraniec, Vasil Khalidov, Pierre Fernandez, Daniel Haziza, Francisco Massa, Alaaeldin El-Nouby, et al. 2023. DINOv2: Learning Robust Visual Features without Supervision. *arXiv preprint arXiv:2304.07193* (2023).
- [41] Junwen Pan, Qi Bi, Yanzhan Yang, Pengfei Zhu, and Cheng Bian. 2022. Label-efficient hybrid-supervised learning for medical image segmentation. In *Proceedings of the AAAI Conference on Artificial Intelligence*, Vol. 36. 2026–2034.
- [42] X. Pan, P. Luo, J. Shi, and X. Tang. 2018. Two at Once: Enhancing Learning and Generalization Capacities via IBN-Net. In *Proceedings of the European Conference on Computer Vision*. 464–479.
- [43] X. Pan, X. Zhan, J. Shi, X. Tang, and P. Luo. 2019. Switchable Whitening for Deep Representation Learning. In *Proceedings of the IEEE/CVF Conference on Computer Vision and Pattern Recognition*. 1863–1871.
- [44] Greg Partyka, James Gridley, and John Lopez. 1999. Interpretational Applications of Spectral Decomposition in Reservoir Characterization. *The leading edge* 18, 3 (1999), 353–360.

- [45] Duo Peng, Yinjie Lei, Munawar Hayat, Yulan Guo, and Wen Li. 2022. Semantic-Aware Domain Generalized Segmentation. In *Proceedings of the IEEE/CVF Conference on Computer Vision and Pattern Recognition*. 2594–2605.
- [46] Duo Peng, Yinjie Lei, Lingqiao Liu, Pingping Zhang, and Jun Liu. 2021. Global and Local Texture Randomization for Synthetic-to-Real Semantic Segmentation. *IEEE Transactions on Image Processing* 30 (2021), 6594–6608.
- [47] Leon N Piotrowski and Fergus W Campbell. 1982. A Demonstration of the Visual Importance and Flexibility of Spatial-Frequency Amplitude and Phase. *Perception* 11, 3 (1982), 337–346.
- [48] Fabrizio J Piva, Daan de Geus, and Gijs Dubbelman. 2023. Empirical Generalization Study: Unsupervised Domain Adaptation vs. Domain Generalization Methods for Semantic Segmentation in the Wild. In *Proceedings of the IEEE/CVF Winter Conference on Applications of Computer Vision*. 499–508.
- [49] Xiaorong Qin, Xinhang Song, and Shuqiang Jiang. 2023. Bi-Level Meta-Learning for Few-Shot Domain Generalization. In *Proceedings of the IEEE/CVF Conference on Computer Vision and Pattern Recognition*. 15900–15910.
- [50] Alec Radford, Jong Wook Kim, Chris Hallacy, Aditya Ramesh, Gabriel Goh, Sandhini Agarwal, Girish Sastry, Amanda Askell, Pamela Mishkin, Jack Clark, et al. 2021. Learning Transferable Visual Models from Natural Language Supervision. In *International Conference on Machine Learning*. PMLR, 8748–8763.
- [51] Aditya Ramesh, Mikhail Pavlov, Gabriel Goh, Scott Gray, Chelsea Voss, Alec Radford, Mark Chen, and Ilya Sutskever. 2021. Zero-Shot Text-to-Image Generation. In *International Conference on Machine Learning*. PMLR, 8821–8831.
- [52] S. R. Richter, V. Vineet, S. Roth, and V. Koltun. 2016. Playing for data: Ground truth from computer games. In *European Conference on Computer Vision (ECCV)*, Vol. 9906. 102–118.
- [53] German Ros, Laura Sellart, Joanna Materzynska, David Vazquez, and Antonio M Lopez. 2016. The Synthia Dataset: A Large Collection of Synthetic Images for Semantic Segmentation of Urban Scenes. In *Proceedings of the IEEE Conference on Computer Vision and Pattern Recognition*. 3234–3243.
- [54] C. Sakaridis, D. Dai, and L. Van Gool. 2021. ACDC: The Adverse Conditions Dataset with Correspondences for Semantic Driving Scene Understanding. In *Proceedings of the IEEE/CVF International Conference on Computer Vision (ICCV)*.
- [55] Mattia Segu, Alessio Tonioni, and Federico Tombari. 2023. Batch Normalization Embeddings for Deep Domain Generalization. *Pattern Recognition* 135 (2023), 109115.
- [56] Yiyou Sun, Yaojie Liu, Xiaoming Liu, Yixuan Li, and Wen-Sheng Chu. 2023. Rethinking Domain Generalization for Face Anti-Spoofing: Separability and Alignment. In *Proceedings of the IEEE/CVF Conference on Computer Vision and Pattern Recognition*. 24563–24574.
- [57] Riccardo Volpi, Hongseok Namkoong, Ozan Sener, John C Duchi, Vittorio Murino, and Silvio Savarese. 2018. Generalizing to Unseen Domains via Adversarial Data Augmentation. *Advances in Neural Information Processing Systems* 31 (2018).
- [58] Jingye Wang, Ruoyi Du, Dongliang Chang, Kongming Liang, and Zhanyu Ma. 2022. Domain Generalization via Frequency-Domain-based Feature Disentanglement and Interaction. In *Proceedings of the 30th ACM International Conference on Multimedia*. 4821–4829.
- [59] Lianzhe Wang, Shiji Zhou, Shanghang Zhang, Xu Chu, Heng Chang, and Wenwu Zhu. 2023. Improving Generalization of Meta-Learning with Inverted Regularization at Inner-Level. In *Proceedings of the IEEE/CVF Conference on Computer Vision and Pattern Recognition*. 7826–7835.
- [60] Zhixiang Wei, Lin Chen, Yi Jin, Xiaoxiao Ma, Tianle Liu, Pengyang Lin, Ben Wang, Huaian Chen, and Jinjin Zheng. 2024. Stronger, Fewer, & Superior: Harnessing Vision Foundation Models for Domain Generalized Semantic Segmentation. In *Proceedings of the IEEE/CVF Conference on Computer Vision and Pattern Recognition*.
- [61] Qi Xu, Liang Yao, Zhengkai Jiang, Guannan Jiang, Wenqing Chu, Wenhui Han, Wei Zhang, Chengjie Wang, and Ying Tai. 2022. DURL: Domain-Invariant Representation Learning for Generalizable Semantic Segmentation. In *Proceedings of the AAAI Conference on Artificial Intelligence*, Vol. 36. 2884–2892.
- [62] Qinwei Xu, Ruipeng Zhang, Ziqing Fan, Yanfeng Wang, Yi-Yan Wu, and Ya Zhang. 2023. Fourier-based augmentation with applications to domain generalization. *Pattern Recognition* 139 (2023), 109474.
- [63] Qinwei Xu, Ruipeng Zhang, Ya Zhang, Yanfeng Wang, and Qi Tian. 2021. A Fourier-based Framework for Domain Generalization. In *Proceedings of the IEEE/CVF Conference on Computer Vision and Pattern Recognition*. 14383–14392.
- [64] Yanchao Yang and Stefano Soatto. 2020. FDA: Fourier Domain Adaptation for Semantic Segmentation. In *Proceedings of the IEEE/CVF Conference on Computer Vision and Pattern Recognition*. 4085–4095.
- [65] Fisher Yu, Wenqi Xian, Yingying Chen, Fangchen Liu, Mike Liao, Vashisht Mahdavan, and Trevor Darrell. 2018. BDD100k: A Diverse Driving Video Database with Scalable Annotation Tooling. *arXiv preprint arXiv:1805.04687* 2, 5 (2018), 6.
- [66] X. Yue, Y. Zhang, S. Zhao, A. Sangiovanni-Vincentelli, K. Keutzer, and B. Gong. 2019. Domain Randomization and Pyramid Consistency: Simulation-to-Real Generalization Without Accessing Target Domain Data. In *Proceedings of the IEEE/CVF International Conference on Computer Vision (ICCV)*. 2100–2110.
- [67] Qiuhaio Zeng, Wei Wang, Fan Zhou, Charles Ling, and Boyu Wang. 2023. Foresee What You will Learn: Data Augmentation for Domain Generalization in Non-Stationary Environment. In *Proceedings of the AAAI Conference on Artificial Intelligence*, Vol. 37. 11147–11155.
- [68] Xingchen Zhao, Chang Liu, Anthony Sicilia, Seong Jae Hwang, and Yun Fu. 2022. Test-time Fourier Style Calibration for Domain Generalization. In *31st International Joint Conference on Artificial Intelligence, IJCAI 2022*. 1721–1727.
- [69] Xingchen Zhao, Niluthpol Chowdhury Mithun, Abhinav Rajvanshi, Han-Pang Chiu, and Supun Samarasekera. 2024. Unsupervised Domain Adaptation for Semantic Segmentation with Pseudo Label Self-Refinement. In *Proceedings of the IEEE/CVF Winter Conference on Applications of Computer Vision*. 2399–2409.
- [70] Yuyang Zhao, Zhun Zhong, Na Zhao, Nicu Sebe, and Gim Hee Lee. 2022. Style-Hallucinated Dual Consistency Learning for Domain Generalized Semantic Segmentation. In *Computer Vision—ECCV 2022: 17th European Conference, Tel Aviv, Israel, October 23–27, 2022, Proceedings, Part XXVIII*. Springer, 535–552.
- [71] Guangtao Zheng, Mengdi Huai, and Aidong Zhang. 2024. AdvST: Revisiting Data Augmentations for Single Domain Generalization. In *Proceedings of the AAAI Conference on Artificial Intelligence*, Vol. 38. 21832–21840.
- [72] Zhun Zhong, Yuyang Zhao, Gim Hee Lee, and Nicu Sebe. 2022. Adversarial Style Augmentation for Domain Generalized Urban-Scene Segmentation. In *Advances in Neural Information Processing Systems*.